Journal of Computational Applied Mechanics 2024, 55(4): 698-710

DOI: 10.22059/jcamech.2024.375372.1053

RESEARCH PAPER

Parametric Blade Generator Incorporating Bézier Surface Principles and Casing Geometry for Optimal Industrial Centrifugal Slurry Pump Design

Shahab Azimi [a,*], Siamak Arzanpour [a], Tim Gjernes [b]

[a] *School of Mechatronics, Simon Fraser University, Surrey Canada*
[b] *Hevvy/Toyo Pumps North America Corporation, Coquitlam Canada*

Abstract

Modern pump and turbomachinery design merges innovative methodologies with computational tools for optimal efficiency and adaptability. This study delves into the intricate design of a parametric blade generator using Bézier curves, renowned for their precision in sculpting smooth, user-defined curves, and offering vast prospects in turbomachinery blade design. Leveraging this precision, our methodology employed eight pivotal anchor points to shape the Bézier surface blade: three at the base, three at the top, and two strategically placed midpoints. These midpoints enhance curvature control, ensuring the blade's form encapsulates the desired aerodynamic and fluid flow properties. Using these eight defined points and four bounding curves, the blade's holistic spatial profile was meticulously drafted. The CAD modeling system, with its advanced loft and guide curve functions, was instrumental in generating the blade surface, resulting in an aerodynamically adept profile optimized for maximum flow efficiency. Beyond the blade, the pump casing geometry was another pivotal focus. Adopting a parametric shape generation for the casing ensured system-wide design coherence, minimizing potential operational bottlenecks and inefficiencies. Classical optimization and iterative refinements were applied to the initial design, with each step analyzed to ensure the final model achieved high performance. Traditional blade design methodologies often offer limited flexibility, confining designers to specific templates and forms. However, this methodology provided greater design flexibility and set a new benchmark in performance optimization. As industries continually evolve and demand more from turbomachinery, the methodologies presented herein will be at the forefront, guiding us into an era of enhanced efficiency, adaptability, and innovation.

Keywords: Computational Fluid Dynamics (CFD), Bézier Curve Parametrization, Pump Performance, Ansys CFX, Dakota Optimization;

[*] Corresponding author;.*E-mail address:*azimi@sfu.ca

1. Introduction

In the competitive landscape of turbomachinery design, achieving efficiency, adaptability, and robustness in pump systems is a critical challenge, especially in the face of complex operational environments. Traditional pump design methods are increasingly proving inadequate, limited by their flexibility and inability to adapt to the varying and complex fluid dynamics of modern applications[1]. This paper introduces an innovative design and optimization methodology that merges advanced geometric design, parametric modeling, computational fluid dynamics (CFD), and state-of-the-art optimization techniques. The focus is on enhancing the performance of centrifugal slurry pumps, which are pivotal in industries from petroleum extraction to waste management.

This study leverages Bézier curve-based parametric blade generation combined with comprehensive pump casing geometry optimization. Special attention is given to slurry pumps, where optimizing blade and casing geometry is essential for handling abrasive and heterogeneous slurry mixtures, aiming to improve performance and durability. The integration of the Dakota† superscript with ANSYS CFX facilitates robust optimization[2] and detailed CFD analysis of the pump model, enabling a sophisticated exploration of the design space and efficient optimization of design parameters.

While the application of Bézier curves in blade design has been explored in turbomachinery[3, 4], the use of Bézier surfaces, known for their enhanced flexibility and versatility, remains significantly underrepresented in the literature[4]. This study aims to bridge this gap by demonstrating the effectiveness of Bézier surface principles in turbomachinery blade design.

The following section, the Literature Review, contextualizes this study within the broader scope of turbomachinery design research. It examines the evolution of design methodologies, particularly focusing on the role of computational tools and Bézier curve principles in advancing pump design technologies.

2. Literature Review

The field of turbomachinery blade design has been intensely influenced by the advent of computational modeling techniques, with Bézier curves playing a pivotal role[5-7]. These curves, known for their precision in computer graphics, have been effectively applied to optimize the aerodynamic profiles of turbomachinery blades. This optimization leads to improved efficiency and performance, a critical factor in the design of effective machinery[8].

Historically, blade design in turbomachinery was constrained by the limitations of traditional methods, which often relied on empirical approaches and simplified geometric models[9, 10]. The introduction of Bézier curves marked a significant shift towards more complex and tailored designs. This shift allowed for greater flexibility and precision in shaping blade profiles, addressing the intricate fluid dynamics challenges inherent in turbomachinery[11, 12].

One of the key advantages of using Bézier curves in blade design is the ability to intricately control the curvature and twist of the blades. This control enables designers to tailor blade geometry to specific operational requirements, resulting in blades that are not only more efficient but also better suited to a variety of challenging environments, such as those found in slurry pumps[13].

The integration of Bézier curve-based design with Computational Fluid Dynamics (CFD) has further enhanced the scope and accuracy of blade design. CFD tools allow for detailed analyses of fluid flow over blade surfaces, providing insights that are crucial for optimizing blade shapes and ensuring they perform as intended in real-world conditions[14].

Looking forward, the application of Bézier curves in turbomachinery blade design is poised for further advancements. The integration of these curves with advanced optimization algorithms and emerging technologies like machine learning promises to revolutionize blade design. This evolution will enable the creation of even more efficient and adaptable turbomachinery, catering to the increasingly complex demands of modern industrial applications.

While Bézier curves have been extensively explored in the context of turbomachinery blade design, the application of Bézier surfaces remains notably underrepresented in current literature. This gap is particularly significant considering the enhanced flexibility and versatility Bézier surfaces offer compared to their curve counterparts. This study seeks to address this gap by exploring the application of Bézier surface principles in the design of turbomachinery blades.

---

† Dakota software facilitates optimization and uncertainty quantification (UQ) in computational models, offering advanced methods for design exploration, risk analysis, and performance validation.

3. Materials and methods

This section provides an in-depth look at the tools and techniques employed in the design and optimization of the pump system. The methodology is a convergence of various advanced tools including Dakota for optimization, ANSYS CFX for Computational Fluid Dynamics (CFD), and SpaceClaim for parametric modeling of the blade and casing. The integration of these tools allows for a comprehensive and iterative approach to pump design, aiming to enhance performance and efficiency.

3.1 Parametric Design using SpaceClaim:

The initial stage in the pump design involves the creation of a parametric model of the pump components, namely the blade and casing. SpaceClaim's 3D CAD software is utilized for its intuitive interface and powerful capabilities in geometry manipulation. In this study, SpaceClaim enables the creation of versatile parametric models, which are essential in exploring various design scenarios and rapidly making modifications based on the optimization results. The blade and casing geometries are parameterized with variables that can be adjusted according to the optimization algorithm's feedback, allowing for a flexible and efficient design process[15].

In the blade shape generation process, we have implemented Bézier curves and surfaces within SpaceClaim's CAD environment through custom coding. This integration introduces a precise mathematical framework for designing complex and customizable shapes[16-18].

In its simplest form, a Bézier curve with three control points creates a quadratic curve. These control points are typically denoted as P_0, P_1 and P_2. The curve is defined by a parametric function that blends these points. For a quadratic Bézier curve, the equation is:

$$B(t) = (1-t)^2 P_0 + 2(1-t)tP_1 + t^2 P_2 \tag{1}$$

Here, t is a parameter that runs from 0 to 1. When $t = 0$, the curve starts at P_0. When $t = 1$, it ends at P_1. The point P_1 influences the curve's shape but is not necessarily on the curve.

On the other hand, a Bézier surface extends the idea of Bézier curves into two dimensions. The simplest form of a Bézier surface is a bilinear patch, which is defined by four control points. However, to create a curved surface, at least eight control points are needed. This setup usually forms a tensor product Bézier surface.

For a Bézier surface with eight control points, the surface is defined by a set of control points P_{ij} where *i* and *j* range over some set of integers. The surface $S(u,v)$ can be expressed as:

$$S(u,v) = \sum_{i=0}^{n} \sum_{j=0}^{m} PijB_i^n(u)B_j^m(v) \tag{2}$$

Here, $B(u)$ and $B(v)$ are the Bernstein polynomials for the respective parameters u and v, which range from *0* to *1*. The indices n and m indicate the degree of the Bézier surface in each parameter direction. The control points P_{ij} define the shape of the surface, with the surface passing near but not necessarily through these points.

In essence, while a Bézier curve is a linear interpolation among control points in a 1D parametric space, a Bézier surface is a bilinear interpolation in a 2D parametric space. Both offer precise control over the shape of curves and surfaces, making them invaluable in graphics and design applications.

Fig 1 showcases two distinct geometric models of a one class of the pump, each created by specifying the positions of eight strategic points in space, along with the number of blades and other parameters of the pump geometry. This groundbreaking technique of blade generation harnesses the strength of Bézier surfaces, providing a strong and adaptable approach to handle intricate blade geometries. The figure exemplifies the versatility of the design, presenting two variations that arise from diverse configurations of the eight control points and number of the blade.

In these models, the Bézier surface serves as the backbone for the blade's profile, smoothly interpolating between the specified control points to form the intricate curvature of the pump blades. The control points are strategically placed to influence the shape, twist, and sweep of the blades, directly impacting the pump's aerodynamic and hydraulic performance. The ability to manipulate these points provides a significant advantage in tailoring the blade geometry to specific operational requirements or optimization objectives.

The Bézier surfaces extend this concept by creating a smooth, continuous surface across the blades, ensuring a coherent and efficient flow path for the fluid. This seamless integration of the blade profiles into a unified surface helps in minimizing flow separation and losses, thereby enhancing the pump's efficiency and performance.

Furthermore, the figure highlights the adaptability of this method in generating a wide range of blade geometries by simply altering the location of the control points and the number of blades. This adaptability is crucial in optimizing the pump design for various applications, from high-efficiency industrial processes to demanding aerospace applications.

By employing Bézier surfaces, this method offers unprecedented control over the blade design, allowing for the creation of highly customized, application-specific pump geometries. The illustrated models in Fig 1are exemplary representations of how computational design tools can significantly advance pump technology, pushing the boundaries of what is possible in terms of performance, efficiency, and adaptability.

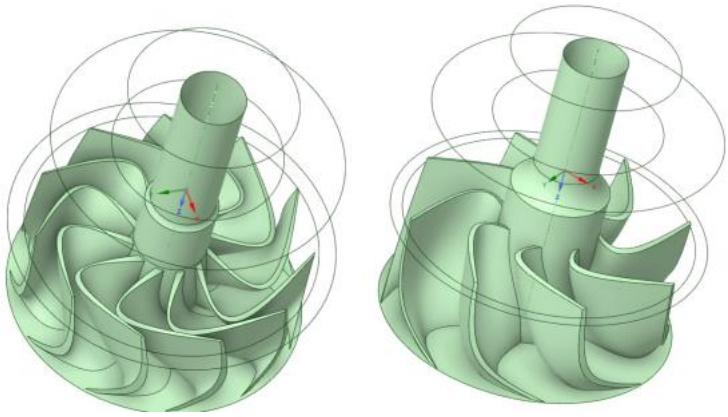

Fig 1: blade shape generation using SpaceClaim and coding the geometry in the model

For the casing geometry of the pump, an integral component dictating the fluid dynamics and overall performance, was meticulously defined, and coded also using SpaceClaim. In our design approach, seven variable parameters (including casing starting and ending radius, two parameters in casing width, starting and ending angles, and casing cone angle – due to the confidentiality of the method the exact parameters not revealed), are utilized to define and manipulate the geometry of the casing in one specific class of the pumps, offering a substantial range of geometric flexibility to optimize the pump's performance. Fig 2 illustrates a sample casing geometry, showcasing the adaptability and precision afforded by these variable parameters.

In the context of the optimization study, these variable parameters are systematically altered to explore a wide design space. This exploration is aimed at identifying casing configurations that yield the best performance in terms of efficiency, reliability, and adaptability to different fluid types and flow rates. The changes in casing geometry directly impact the flow domain, affecting the velocity profiles, pressure distributions, and potential recirculation zones within the pump. Therefore, careful and informed manipulation of these parameters is crucial to achieving an optimal design.

3.2 CFD Analysis with ANSYS CFX:

Following the parametric design phase, the models are subjected to a rigorous CFD analysis using ANSYS CFX. This software is selected for its robustness and accuracy in simulating fluid flow and heat transfer in complex geometries and flow conditions. The stage (mixing plane) methodology is employed to simulate the steady-state interaction between the rotating blade and the fluid, providing insight into the performance implications of different design configurations. The CFD simulations are critical in evaluating the aerodynamic and hydraulic performance of the pump, including parameters such as pressure distribution, flow velocity, and turbulence intensity.

Fig 3 provides a detailed visualization of the simulation domain as configured in ANSYS CFX. This figure captures the comprehensive setup for the CFD simulation, which is conducted in steady-state mode using liquid water as the working fluid. The simulation domain encompasses the intricate geometry of the pump, including the impeller, casing, and flow passages, all meticulously modeled to reflect the actual physical characteristics of the pump.

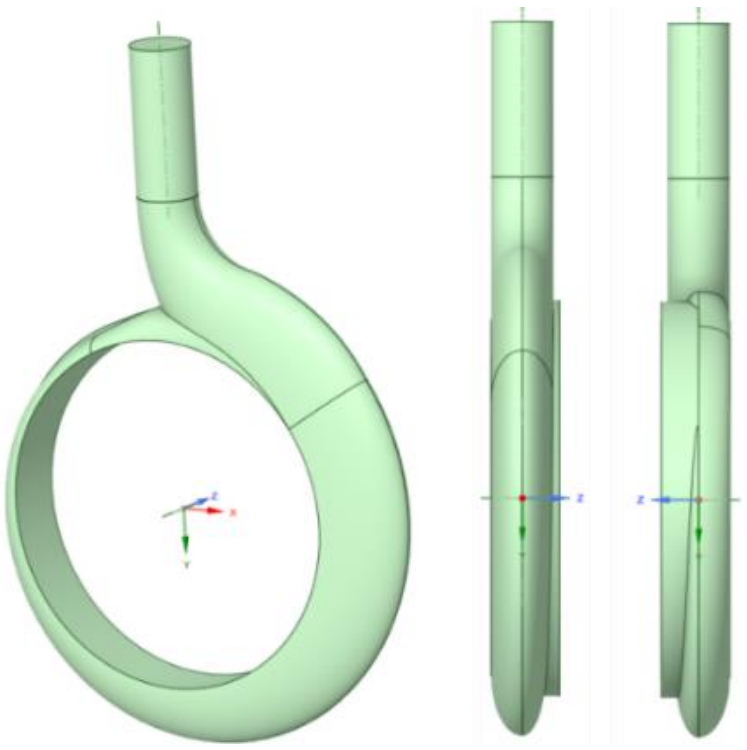

Fig 2: sample casing (shown from different perspectives) for design optimization

In setting up the CFD simulation, several assumptions and selections are made to accurately capture the fluid dynamics within the pump while ensuring computational efficiency. Firstly, the effect of gravity is neglected. This assumption is typical in such simulations where the primary interest is in understanding the fluid flow induced by the pump itself, and the influence of gravity on the overall flow pattern is minimal or irrelevant.

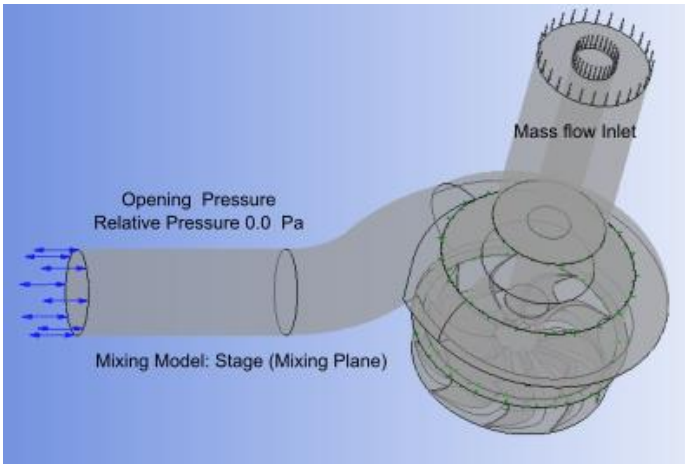

Fig 3: CFD domain and the boundary conditions in Ansys CFX

The Shear Stress Transport (SST) turbulence model is employed, recognized for its accuracy and robustness in predicting the onset and amount of turbulence in various flow regimes, particularly those prevalent in turbomachinery applications[19, 20]. The SST model combines the best of k-omega and k-epsilon models in near-wall and far-field regions, respectively, providing a comprehensive depiction of the turbulent characteristics of the flow. Alongside this, automatic wall functions are utilized to resolve the flow near the walls of the pump. These functions are critical in capturing the boundary layer effects accurately without the excessive computational cost of resolving every detail of the flow near the wall[21].

It is also noted that heat transfer effects are not considered in the simulation. This decision is guided by the focus of the study on the hydraulic and aerodynamic performance of the pump, where the primary interest lies in

understanding the flow patterns, pressure distributions, and overall fluid dynamics. By omitting the heat transfer simulation, the computational resources are more focused on these aspects, providing a more refined and accurate analysis of the flow characteristics crucial for optimizing pump performance.

ANSYS-CFX incorporates fluid dynamics principle to solve the flow domain equations and particle behavior which were the theory of this research. Navier–Stokes equations define the Newtonian flow domain behavior, which uses the conservation of mass, momentum (Newton's second law), as expressed in the following equations[22].

Conservation of mass:

$$\frac{\partial \rho}{\partial t} + \nabla \cdot (\rho \mathbf{V}) = 0 \tag{3}$$

Momentum in X, Y, and Z-direction.

$$\begin{aligned}
\frac{\partial (\rho u)}{\partial t} + \nabla \cdot (\rho u \mathbf{V}) &= -\frac{\partial P}{\partial x} + \frac{\partial \tau_{xx}}{\partial x} + \frac{\partial \tau_{yx}}{\partial y} + \frac{\partial \tau_{zx}}{\partial z} + \rho f_x \\
\frac{\partial (\rho v)}{\partial t} + \nabla \cdot (\rho v \mathbf{V}) &= -\frac{\partial P}{\partial y} + \frac{\partial \tau_{xy}}{\partial x} + \frac{\partial \tau_{yy}}{\partial y} + \frac{\partial \tau_{zy}}{\partial z} + \rho f_y \\
\frac{\partial (\rho w)}{\partial t} + \nabla \cdot (\rho w \mathbf{V}) &= -\frac{\partial P}{\partial z} + \frac{\partial \tau_{xz}}{\partial x} + \frac{\partial \tau_{yz}}{\partial y} + \frac{\partial \tau_{zz}}{\partial z} + \rho f_z
\end{aligned} \tag{4}$$

The velocity of flow along the X, Y, and Z-axes are represented by u, v, and w respectively, the static pressure of the flow and density of the fluid are shown by P and ρ respectively. Moreover, the viscous stresses are represented by τ.

The Shear Stress Transport (*SST*) k-ω turbulence model was utilized in ANSYS-CFX for simulating flow regimes spanning laminar, transitional, and fully turbulent states. This model represents a fusion of the standard k-ω model within the near-wall vicinity and the k-ε model in the far-field region[23]. Extensive research demonstrates that the *SST* k-ω turbulence model accurately forecasts transitional turbulence flows[24, 25]. In such cases involving a range from laminar to turbulent flows, the Reynolds-averaged Navier-Stokes equations (RANS) are frequently employed to outline the conservation of mass and momentum:

$$\frac{\partial (\rho k)}{\partial t} + \frac{\partial (\rho U_j k)}{\partial x_j} = \frac{\partial}{\partial x_j}\left[\left(\mu + \frac{\mu_t}{\sigma_k}\right)\frac{\partial k}{\partial x_j}\right] + P_k - \beta' \rho k \omega + P_{kb} \tag{5}$$

$$\frac{\partial (\rho \omega)}{\partial t} + \frac{\partial (\rho U_j \omega)}{\partial x_j} = \frac{\partial}{\partial x_j}\left[\left(\mu + \frac{\mu_t}{\sigma_\omega}\right)\frac{\partial \omega}{\partial x_j}\right] + \alpha \frac{\omega}{k} P_k - \beta \rho \omega^2 + P_{\omega b} \tag{6}$$

Where, β', α, β, σ_k, and σ_ω are constant. The buoyancy production, P_{kb} for full buoyancy model and Boussinesq buoyancy model are shown in Equation 6 and 7 respectively.

$$P_{kb} = -\frac{\mu_t}{\rho \sigma_\rho} g_i \frac{\partial \rho}{\partial x_i}, \quad \sigma_\rho = 1 \tag{7}$$

$$P_{kb} = -\frac{\mu_t}{\rho}\beta g_i \frac{\partial T}{\partial x_i}, \quad \sigma_\rho = 0.9 \tag{8}$$

Where $P_{\omega b}$ is:

$$P_{\omega b} = \frac{\omega}{k}\left((\alpha+1)C_3 \max(P_{kb}, 0) - P_{kb}\right) \tag{9}$$

3.3 Optimization

3.3.1 Optimization definition and goal

The optimization process is carefully implemented on both the blade geometry and the casing of the pump, utilizing a comprehensive set of design parameters to refine the geometries towards optimal performance. Specifically, the blade geometry is defined by 22 continuous variable design parameters that dictate the shape and characteristics of the Bézier surface, intricately controlling the curvature and twist of the blades for enhanced aerodynamic efficiency. Additionally, one discrete integer variable is employed to determine the number of blades, allowing for the exploration of different blade configurations and their impact on pump performance.

For the casing, 7 continuous variable parameters are identified and systematically adjusted to fine-tune the casing geometry. These parameters influence critical aspects of the casing design, such as the volute shape, and wall curvature, directly affecting the flow distribution and hydraulic efficiency of the pump.

All design variables, both for the blade and casing, are constrained within realistic and practical ranges to ensure the feasibility of the resulting designs. The limitations on these variables were carefully defined to construct a classical optimization problem, encapsulating a total of 30 design parameters. This setup allows for a robust and systematic exploration of the design space, ensuring that the optimization process is both comprehensive and targeted towards viable, high-performance pump configurations.

The optimization seeks to navigate this high-dimensional design space efficiently, identifying configurations that meet or exceed performance criteria while adhering to the constraints imposed. The resulting designs are expected to represent significant advancements in pump technology, offering improved efficiency, and adaptability to various operational conditions.

By employing such an extensive and carefully orchestrated optimization process, the study aims to push the boundaries of pump design, leveraging the full potential of computational design tools and advanced optimization techniques to achieve superior performance characteristics.

3.3.2 Optimization Methodology

The Efficient Global Optimization (EGO) methodology forms the cornerstone of the optimization process in this study. EGO is particularly suited for the unconstrained minimization of complex and expensive-to-evaluate functions, which is often the case in advanced turbomachinery design. This section outlines the theory behind EGO in a simplified manner, focusing on its application in the optimization of the pump design[26].

3.3.2.1 Gaussian Process Model:

The foundation of EGO is the construction of an initial Gaussian Process (GP) model as a global surrogate for the response function. A GP model is a probabilistic model that predicts not only the expected output for a given input but also the uncertainty of the prediction. It assumes that the outputs for similar inputs will be close to each other, with the degree of similarity determined by a covariance function. The GP model is updated iteratively with new data points, improving its accuracy, and reducing uncertainty in regions of interest in the design space.

3.3.2.2 Expected Improvement Function (EIF):

The selection of new data points to update the GP model is guided by the Expected Improvement Function (EIF). The EIF is a strategy that quantifies the expected reduction in the objective function if a new sample point is added to the model. It balances the need to explore new regions of the design space (where the model is uncertain) and to

exploit the regions that are likely to offer improvements (where the model predicts better outcomes). This balance ensures that the optimization process does not get stuck in local minima and progresses towards the global optimum.

3.3.2.3 Optimization Procedure:

The general procedure for EGO involves the following steps:

1. Initial Model Creation: Build an initial Gaussian process model of the objective function based on available data.
2. Optimization Iteration:
3. Find the point that maximizes the EIF.
4. If the maximum EIF value is below a predefined threshold, indicating that further improvement is minimal, the optimization concludes.
5. Otherwise, evaluate the objective function at the new point and update the GP model with this information. Repeat this step until the stopping criterion is met.

The use of EGO in this study allows for a systematic and efficient exploration of the complex design space associated with the pump's blade and casing geometry. By iteratively refining the model and focusing the search on promising regions, EGO drives the design towards optimal performance characteristics.

3.4 Integration and Iterative Workflow:

The integration of SpaceClaim, ANSYS CFX, and Dakota is central to the methodology. The iterative workflow begins with the parametric design in SpaceClaim, followed by CFD analysis in ANSYS CFX to evaluate the current design's performance. The results are then fed into Dakota, which adjusts the design parameters based on the optimization objectives and constraints. This cycle repeats, with each iteration refining the design closer to the optimal solution. The iterative process continues until the improvements become marginal or the optimal solution is reached according to the predefined criteria.

3.5 Validation and Analysis:

Upon completion of the optimization cycle, the final design is validated through additional CFD simulations and, if possible, experimental tests. The validation process ensures that the optimized design meets the desired performance objectives and adheres to operational constraints. A thorough analysis is conducted to compare the optimized design with the baseline model, highlighting the improvements achieved and discussing potential implications for real-world applications.

The Grid Convergence Method (GCM), based on the Richardson Extrapolation (RE) technique, was used to verify the precision of our findings and to assess mesh independence. This approach enhances the accuracy of numerical solutions by examining them at different grid sizes. The objective is to attain a solution that would be equivalent to one achieved with an infinitely small grid. This method systematically computes solutions on grids of varying resolutions and evaluates the errors between them[27, 28].

4. Results and discussion

To confirm the accuracy of our simulation methodology, we began with a comparison between experimental results and simulation data for the original pump at a specific class. Fig 4 illustrates the correlation between efficiency (E) and flow rate as a fraction of the maximum capacity (Q Max). The simulation curve for the original design is plotted alongside the corresponding experimental data, serving as a foundational step in validating our computational approach.

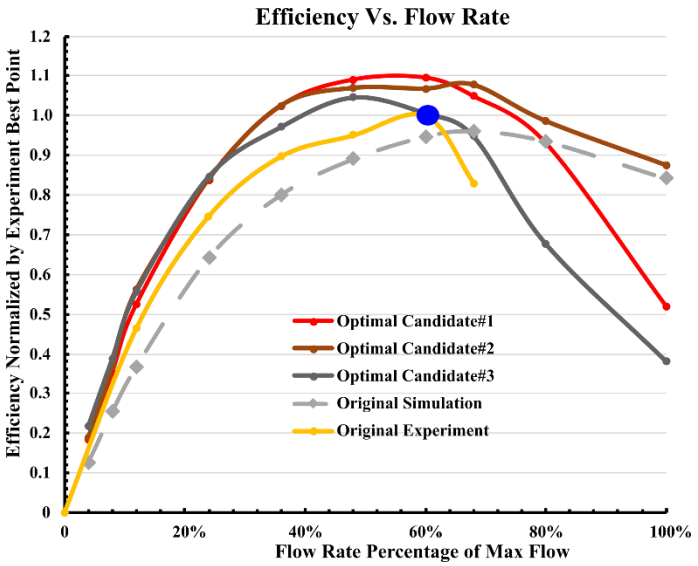

Fig 4: efficiency comparison of the original pump design and three optimized candidates across a range of flow rates.

This graph demonstrates that the original pump simulation data is in close alignment with the experimental results, particularly within the mid-range flow rates. This overlap supports the validity of the simulation process, signifying that the computational model is capable of accurately emulating the physical behaviors of the pump across a variety of operational conditions. Additionally, the depicted efficiency curves for the optimal candidates indicate an approximate 10% enhancement in performance efficiency.

In evaluating the reliability of our simulations, we conducted a grid independence analysis by examining the effects of varying mesh element sizes on the outcomes, employing the Richardson Extrapolation Method (REM). Three mesh sizes were selected for this purpose: a fine mesh (4 mm), a medium mesh (6 mm), and a coarse mesh (10 mm), with respective indices of 0.0068, 0.0093, and 0.0135. For this investigation, Candidate 1 was chosen as the subject for the grid independence study. To analyze the axial velocity profile in this candidate, a plane (line) was established at three diameters below the domain outlet boundary. As it is depicted in Fig 5. different mesh parameters were used to calculate both the average apparent parameter (*P*ave) and the Grid Convergence Index (GCI). As shown in Fig 6, the results revealed that the average apparent parameter (*P*ave) is 3.25, with a GCI of 1.48% for the fine mesh, while these are 4.38 and 2.25% for the medium mesh. These findings highlight the consistency of our simulations across different mesh sizes[28].

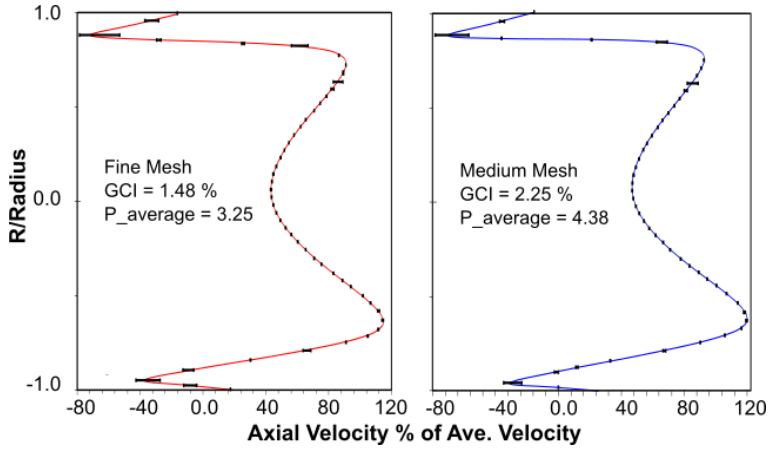

Fig 5: grid independency study for the simulation with Richardson extrapolation method

Upon establishing the validity of the simulation methodology, the study introduces three optimized candidates, each representing a different design iteration aimed at enhancing the pump's efficiency. Notably, all three candidates demonstrate a marked improvement in efficiency, exceeding a 10 percent increase at certain operational points when compared to the original pump design, as compared in Fig 4. Considering these comparison, it is concluded that:

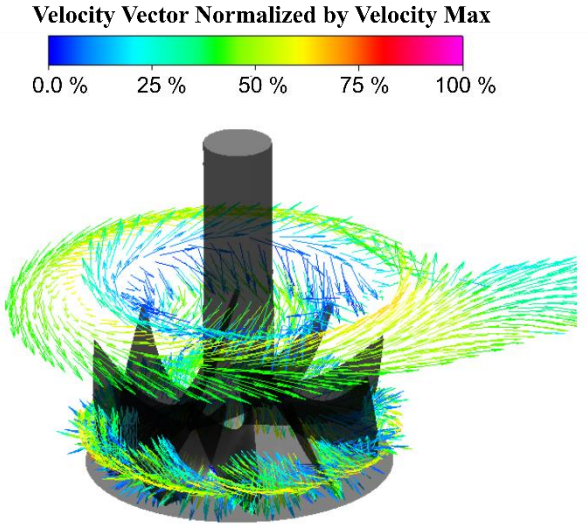

Fig 6: flow vectors on two different planes on optimal Candidate #1.

Optimal Candidate #1 presents a substantial increase in efficiency across a broad range of flow rates, peaking at just over 40 percent of Q Max. This design iteration appears to offer the most significant enhancement in efficiency, particularly in the most commonly utilized operational range, suggesting that the design modifications in blade and casing geometries contribute positively to the fluid dynamics within the pump.

Optimal Candidate #2 maintains a similar efficiency profile to the original pump but extends the range of high-efficiency operation. The peak efficiency is slightly lower than that of Candidate #1; however, the broader high-efficiency range may provide better performance over varied operational conditions, which could be advantageous in applications with fluctuating demand.

Optimal Candidate #3 shows an intriguing efficiency profile with a distinct peak that surpasses the original design, yet it exhibits a steep decline as the flow rate approaches 100 percent of Q Max. This suggests that while the design changes incorporated in this candidate can yield high efficiency, they might be optimized for a narrower operational range. Such a design could be suitable for specialized applications where the pump operates within a specific flow rate window.

Fig 6 focuses on the flow dynamics around the impeller blades for optimal candidate # 1 at two critical cross-sections: one passing through the mid-section of the casing and another positioned above the blades. The visualization captures the velocity vectors, with the color gradient—from blue to red—representing the velocity magnitude as a percentage of the maximum observed in the system, where blue signifies the lowest and red the highest velocities. In the cross-section passing through the mid-section of the casing, we observe the interaction of the fluid with the impeller blades, providing insights into the flow patterns that contribute to the pump's efficiency. The streamlines above the blades offer a top-down perspective, crucial for evaluating the clearance flow and the potential for recirculation or energy losses.

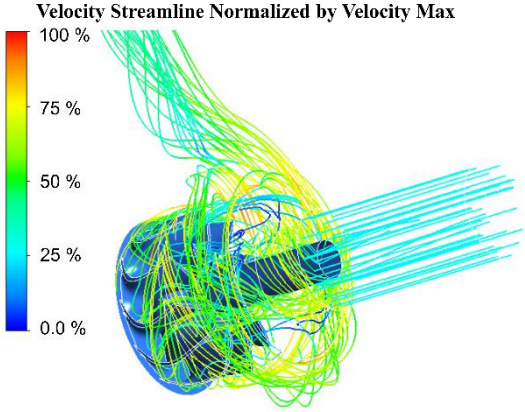

Fig 7: flow streamline on optimal design Candidate #2

Fig 7 illustrates coherent streamlines emanating from the impeller in the optimal candidate #2 in which demonstrates an efficient fluid exit path, which is indicative of a potentially optimized design for reduced turbulence and improved hydraulic performance.

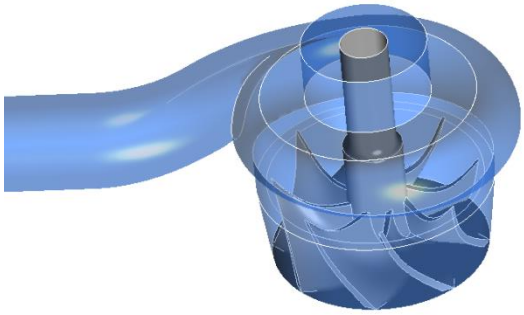

Fig 8: optimal casing and blade geometry for optimal Candidate #3

Fig 8 presents the CAD geometry of candidate #3 in conjunction with its corresponding optimal casing. This configuration has been determined to achieve higher efficiency relative to the original design. The detailed representation allows for a comprehensive evaluation of the blade contours and casing dimensions, which have been meticulously refined to enhance the pump's performance. This illustration is pivotal to understanding the modifications that contribute to the improved hydraulic efficiency of the system.

In summary, the optimized candidates underscore the potential of using advanced simulation and optimization techniques to significantly enhance pump efficiency. The improved designs suggest that even small alterations in blade and casing parameters can have a profound impact on pump performance. These findings not only validate the employed simulation methodology but also open avenues for further design refinements. Future work may focus on exploring the trade-offs between efficiency peaks and operational range, aiming to develop pumps that can deliver high efficiency across a wider spectrum of conditions.

5. Conclusion

While the precise metrics detailing the reduction in design iteration times and the decrease in the necessity for physical prototype testing remain qualitative, it is evident that the use of advanced simulation and optimization tools has led to a substantial improvement in design efficiency. The primary quantitative outcome, a 10% increase in efficiency, is a significant testament to the effectiveness of the methodologies employed.

It is important to note the qualitative benefits that have emerged from this approach. The advanced simulation capabilities have enabled us to evaluate potentially thousands of virtual designs—a process that would be logistically and economically unfeasible with physical prototypes. In practice, while we might physically test several prototypes, the simulations afford us the ability to perform exhaustive iterative design work, which considerably enhances the potential for optimal performance in the final product.

This approach has significantly reduced the time required for design iterations, not merely by eliminating the need for multiple physical tests but also by allowing for a rapid and extensive exploration of the design space. This has not only accelerated the development process but also reduced costs and resources traditionally associated with physical testing.

The enhanced capability to custom-design pumps through the Bézier surface methodology further underscores the study's success. By incorporating these advanced design and optimization tools, we have not only validated the simulation methodology against experimental benchmarks but have also realized a remarkable leap in pump design efficiency.

Thus, the overarching benefit of this study is twofold: it offers substantial time savings in the design iteration process and provides the unparalleled ability to test a vast array of virtual prototypes, culminating in the selection of an optimal design. This dual advantage underscores the transformative potential of our methods for future turbomachinery design and optimization endeavors.

Acknowledgements

The authors gratefully acknowledge the financial support provided by the Natural Sciences and Engineering Research Council of Canada and the Hevvy/Toyo Pumps North America Corporation. This funding has been crucial in facilitating the research and development activities presented in this study. We extend our sincere thanks for their commitment to advancing scientific and engineering research.

References

[1] K. Alawadhi, B. Alzuwayer, T. A. Mohammad, M. H. Buhemdi, Design and optimization of a centrifugal pump for slurry transport using the response surface method, *Machines*, Vol. 9, No. 3, pp. 60 %@ 2075-1702, 2021.

[2] B. M. Adams, W. J. Bohnhoff, K. R. Dalbey, M. S. Ebeida, J. P. Eddy, M. S. Eldred, R. W. Hooper, P. D. Hough, K. T. Hu, J. D. Jakeman, Dakota, a multilevel parallel object-oriented framework for design optimization, parameter estimation, uncertainty quantification, and sensitivity analysis: version 6.13 user's manual, Sandia National Lab.(SNL-NM), Albuquerque, NM (United States), 2020.

[3] D. Song, S. H. Kang, Y. Kim, S. J. Shin, Turbine blade structural analysis by using the isogeometric Bernstein-Bezier discretization, in *Proceeding of*, 2574.

[4] R. Nanthini, B. Prasad, Y. Sanyasiraju, Effect of Bezier control points on blade pressure distribution, in *Proceeding of*, AIP Publishing, pp.

[5] T. S. Rengma, M. K. Gupta, P. M. V. Subbarao, A novel method of optimizing the Savonius hydrokinetic turbine blades using Bezier curve, *Renewable Energy*, Vol. 216, pp. 119091 %@ 0960-1481, 2023.

[6] H. Zhang, L. Tang, Y. Zhao, Influence of blade profiles on plastic centrifugal pump performance, *Advances in Materials Science and Engineering*, Vol. 2020, No. 1, pp. 6665520 %@ 1687-8442, 2020.

[7] V. G. Gribin, A. A. Tishchenko, R. A. Alekseev, V. A. Tishchenko, I. Y. Gavrilov, V. V. Popov, A method for parametrically representing the aerodynamic profiles of axial turbine machinery blades, *Thermal Engineering*, Vol. 67, pp. 422-429 %@ 0040-6015, 2020.

[8] J. Schiffmann, Integrated design and multi-objective optimization of a single stage heat-pump turbocompressor, *Journal of Turbomachinery*, Vol. 137, No. 7, pp. 071002 %@ 0889-504X, 2015.

[9] N. P. Jaiswal, CFD analysis of centrifugal pump: a review, *Journal of Engineering Research and Applications*, Vol. 4, pp. 175-178, 2014.

[10] C. C. Xia, Y. J. Gou, S. H. Li, W. F. Chen, C. Shao, An automatic aerodynamic shape optimisation framework based on DAKOTA, in *Proceeding of*, IOP Publishing, pp. 012021 %@ 1757-899X.

[11] J. G. Marshall, M. Imregun, A review of aeroelasticity methods with emphasis on turbomachinery applications, *Journal of fluids and structures*, Vol. 10, No. 3, pp. 237-267 %@ 0889-9746, 1996.

[12] F. Gagliardi, Shape Parameterization and Constrained Aerodynamic Optimization. Applications Including Turbomachines, 2020.

[13] T. Capurso, L. Bergamini, M. Torresi, A new generation of centrifugal pumps for high conversion efficiency, *Energy Conversion and Management*, Vol. 256, pp. 115341 %@ 0196-8904, 2022.

[14] D. Harish, R. D. Bharathan, S. Kapil, S. V. Ramana Murthy, D. Kishore Prasad, Aerodynamic Design of Axial Flow Turbine for a Small Gas Turbine Engine, in *Proceeding of*, Springer, pp. 99-111.

[15] G. E. Farin, 2002, *Curves and surfaces for CAGD: a practical guide*, Morgan Kaufmann,

[16] P. Les, T. Wayne, The NURBS book, *Monographs in Visual Communication, Springer Series*, 1997.

[17] D. F. Rogers, 2000, *An introduction to NURBS: with historical perspective*, Elsevier,

[18] H. Prautzsch, W. Boehm, M. Paluszny, 2002, *Bézier and B-spline techniques*, Springer,

[19] E. Casartelli, L. Mangani, D. Roos Launchbury, A. Del Rio, Application of advanced RANS turbulence models for the prediction of turbomachinery flows, *Journal of Turbomachinery*, Vol. 144, No. 1, pp. 011008 %@ 0889-504X, 2022.

[20] R. Balasubramanian, S. Barrows, J. Chen, Investigation of shear-stress transport turbulence model for turbomachinery applications, in *Proceeding of*, 566.

[21] S. Rajendran, K. Purushothaman, Analysis of a centrifugal pump impeller using ANSYS-CFX, *International Journal of Engineering Research & Technology*, Vol. 1, No. 3, pp. 1-6, 2012.

[22] F. R. Menter, R. Sechner, A. Matyushenko, Best Practice: RANS Turbulence Modeling in Ansys CFD, Ansys, Inc, 2021.

[23] F. R. Menter, M. Kuntz, R. Langtry, Ten years of industrial experience with the SST turbulence model, *Turbulence, heat and mass transfer*, Vol. 4, No. 1, pp. 625-632, 2003.

[24] G. Guo, R. Zhang, H. Yu, Evaluation of different turbulence models on simulation of gas-liquid transient flow in a liquid-ring vacuum pump, *Vacuum*, Vol. 180, pp. 109586 %@ 0042-207X, 2020.

[25] M. Ennouri, H. Kanfoudi, A. Bel Hadj Taher, R. Zgolli, Numerical flow simulation and cavitation prediction in a centrifugal pump using an SST-SAS turbulence model, *Journal of Applied Fluid Mechanics*, Vol. 12, No. 1, pp. 25-39 %@ 1735-3572, 2019.

[26] R. Lavimi, A. E. Benchikh Le Hocine, S. Poncet, R. Panneton, B. Marcos, Centrifugal blower optimization using gradient-free approaches and RANS simulation, in *Proceeding of*, 3313.

[27] K. M. Almohammadi, D. B. Ingham, L. Ma, M. Pourkashan, Computational fluid dynamics (CFD) mesh independency techniques for a straight blade vertical axis wind turbine, *Energy*, Vol. 58, pp. 483-493 %@ 0360-5442, 2013.

[28] I. Celik, O. Karatekin, Numerical experiments on application of Richardson extrapolation with nonuniform grids, 1997.